International Journal of Science and Research (IJSR)
ISSN: 2319-7064
Impact Factor 2025: 7.089

# Integrating Geospatial and Machine Learning Techniques for Landslide Mitigation and Risk Assessment in Mizoram, India

**Joel TC Vanlalnunzira[1], Satya Prakash[2]**

[1]Department of Civil Engineering, National Institute of Technology, Mizoram, India
Corresponding Author Email: dt23ce001[at]nitmz.ac.in
ORCID: 0009-0008-0724-5146

[2]Department of Civil Engineering, Sharda University, Greater Noida, Uttar Pradesh, India
Email: *satya.prakash[at]sharda.ac.in*
ORCID: 0000-0001-6633-7480

**Abstract:** ***This study addresses landslide susceptibility in Mizoram, India, a region characterized by steep terrain and high rainfall. The objective is to improve risk prediction using an integrated geospatial and machine learning framework. Fifteen conditioning factors, including topographic, geological, hydrological, and land-use variables, were analysed using GIS and remote sensing data. Machine learning models such as Random Forest, Gradient Boosting Decision Tree, Extreme Gradient Boosting, and stacking ensembles were trained on historical landslide data using an 80:20 train-test split. Model performance was evaluated using accuracy, AUC, RMSE, and Kappa index. The XGB-based models achieved the highest predictive performance with AUC values above 0.90 and reduced error metrics. The resulting landslide susceptibility maps were integrated with population and infrastructure data to assess regional risk. The findings support improved land-use planning and disaster mitigation strategies, contributing to enhanced resilience in landslide-prone regions.***

**Keywords:** Landslide susceptibility mapping, GIS-based modelling, XGBoost, machine learning, ROC analysis, Mizoram, Risk assessment

## 1. Introduction

Landslides triggered by heavy rainfall pose a serious threat to both lives and property, particularly in areas experiencing rapid urbanization and infrastructure expansion. As cities grow, the demand for new housing and roads increases, making landslides an even greater risk (Yalcin and Bulut, 2007) Unlike floods, which often allow for rebuilding and recovery, landslides can cause irreversible destruction, leaving lasting impacts on affected communities (Alejandrino et al., 2016). They also disrupt economic activities by blocking key transportation routes, particularly during the monsoon season when landslides are most common. Between 2011 and 2019, thousands of landslides were recorded in the study area, with most occurring during the monsoon months. While human activities contribute to some of these events, their effects are generally overshadowed by natural triggers such as intense rainfall, seismic activity, and deforestation (Aversa et al., 2016). Areas receiving high annual rainfall—ranging from 2500mm to 3200mm—are particularly vulnerable, as excessive moisture weakens soil stability and increases the likelihood of slope failure (Sengupta and Nath, 2022). To reduce the risks associated with landslides, practical disaster prevention strategies are essential. One of the most effective approaches is landslide susceptibility mapping (LSM), which plays a key role in disaster risk reduction, especially when combined with Geographic Information Systems (GIS) (Yuke et al., 2022). Conducting a thorough analysis of landslide-prone areas provides valuable insights that can help mitigate future hazards. Recent advancements in satellite remote sensing and the increasing availability of high-resolution geospatial data have significantly improved the accuracy of these assessments (Bhusan et al., 2013). GIS-based modeling allows researchers to analyze and visualize multiple landslide-triggering factors, making risk assessment more precise. Over the years, several studies have been conducted to assess landslide risks in the study area, and recent efforts in micro-zonation have helped classify landslide-prone regions more effectively.

The main objective of this study is to develop a robust landslide susceptibility model using integrated geospatial and machine learning techniques and to evaluate regional risk by combining susceptibility results with population density and infrastructure exposure. This study uses machine learning techniques to develop a detailed landslide susceptibility map (LSM). It also emphasizes the risk assessment of population in various district and various infrastructures inside Mizoram state against the landslide susceptible areas incorporating Landslide Susceptibility Map generated. The findings provide crucial insights for identifying high-risk areas and strengthening disaster management strategies. Moreover, the susceptibility map is expected to serve as a valuable resource for highway engineers, geologists, and policymakers involved in infrastructure planning. By incorporating these findings, authorities can make more informed decisions and implement proactive measures to reduce landslide risks and enhance community resilience.

### 1.1 Study Area

The study area, shown in Fig. 1, is situated in the southern region of Northeast India, extending between longitudes 92°39'54" E to 92°46'57" E and latitudes 23°39'54" N to 23°50'35" N. This region is characterized by hilly terrain and receives an average annual rainfall ranging from 2500 mm to 3000 mm. Aizawl is covered by Survey of India toposheet numbers 83 A/9, 83 A/10, and 83 A/84. The geographical expanse of Aizawl is approximately 120.3 km$^2$. Geologically,

the area spans the Pre-Cambrian to Quaternary epochs. The dominant rock formations are sandstone and shale, both common tertiary rocks that weather into platy and splintery surfaces, making them prone to landslides. These rock formations are part of the Disang and Barail groups. The region is not only geologically active but is also classified as seismogenic, falling within Seismic Zone V. According to BIS (2002), the area frequently experiences moderate to high-magnitude earthquakes, leading to significant damage to infrastructure and loss of human lives (Sengupta and Nath, 2022).

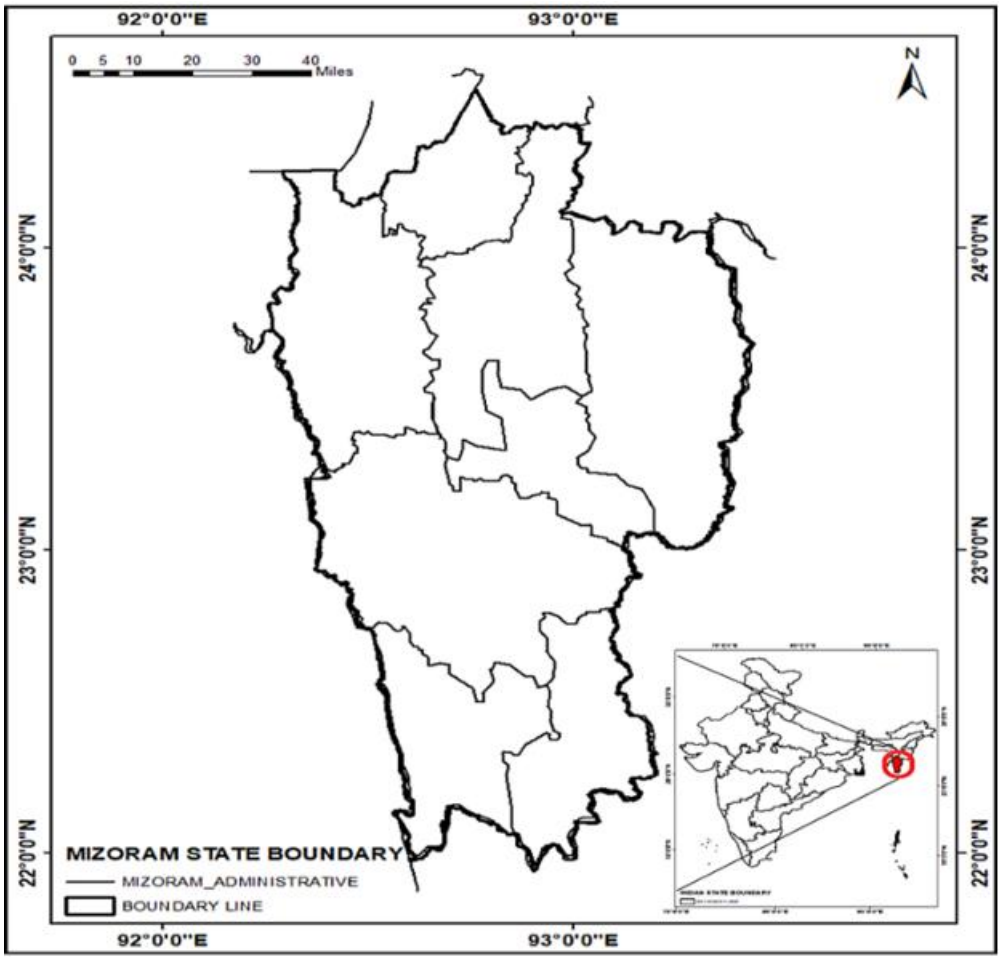


**Figure 1:** Study Area

## 2. Methodology

### 2.1 Modelling Approach

Various datasets were gathered from multiple sources based on a review of relevant literature. Key sources included GIS-Bhukosh, USGS, Google Earth Engine Sentinel-2, and station data from the Mizoram Remote Sensing Application Centre (MIRSAC). From these sources, a total of fifteen landslide conditioning factors—along with a landslide inventory—were compiled for analysis. To process these datasets, ArcGIS software was used to extract the necessary information for further study. To ensure the reliability of the data, a multicollinearity test was performed using a Correlation Matrix and Variance Inflation Factor (VIF). This step helped identify any outliers or highly correlated variables that could affect the accuracy of the results. Once the datasets were refined and verified, they were integrated into various machine learning models to assess landslide susceptibility.

### 2.2 Landslide Conditioning Factors

This study utilized fifteen conditioning factors to generate a landslide susceptibility zonation map, drawing on insights from previous research (Bhusan et al., 2013; Sengupta and Nath, 2022). The data for these factors were collected from multiple sources. The Digital Elevation Model (DEM) was obtained from the USGS website, where four segmented models were merged within a GIS environment using ArcMap software. Additional datasets, including rainfall, lithology, geomorphology, lineaments, proximity to earthquake zones, and road networks, were sourced from the Geological Survey of India. Land Use/Land Cover (LULC) and the Normalized Difference Vegetation Index (NDVI) were derived from Sentinel data available on the ESRI satellite imagery platform via Google Earth Engine.

Elevation plays a crucial role in landslide occurrence, as higher elevations typically have steeper slopes, increasing the chances of slope failure (Pourghasemi et al., 2012; Pradhan, 2010). In regions with fragile geological conditions, such as Mizoram—where elevations reach up to 2,100 meters above mean sea level (MSL)- landslides are frequent, particularly during the monsoon season or following seismic activity. Slope aspect, or the direction a slope faces, also influences

landslide susceptibility. North- and east-facing slopes tend to retain more moisture due to reduced solar exposure, making them more prone to failure (Huang et al., 2017; Zhu and Huang, 2006). In contrast, south- and west-facing slopes receive more sunlight, leading to drier conditions and lower landslide risks (Catani et al., 2005). Similarly, hill shading impacts landslide likelihood, as shaded slopes retain more moisture, increasing instability (Dai and Lee, 2002; Shahabi et al., 2013)

Slope curvature is another important factor. Convex slopes, which curve outward, tend to accumulate rainwater, making the soil heavier and less stable (Nefeslioglu et al., 2008). On the other hand, concave slopes facilitate water drainage, reducing landslide risk (Shahabi et al., 2013). Mizoram's varied geomorphology, characterized by diverse hill orientations and altitudes, results in differences in landslide susceptibility across the state. Lithology, or rock composition, is another critical determinant of slope stability. The weak sedimentary rocks that dominate Mizoram break down easily under weathering, increasing the likelihood of landslides (Sengupta and Nath, 2022). Proximity to geological faults and fractures, known as lineaments, further contributes to landslide risk, as tectonic activity can destabilize (Thai Pham et al., 2018; Tien Bui et al., 2012). Given that Mizoram lies within the Indo-Burmese thrust zone, it is particularly vulnerable to earthquake-induced landslides.

Infrastructure development also plays a significant role in triggering landslides. Road construction, in particular, has altered the natural flow of water and increased soil instability in many parts of the state (Sengupta and Nath, 2022). The construction of national highways and railway projects has contributed to this issue, as some projects proceed without adequate slope stabilization measures (Saadatkhah et al., 2015). Additionally, shifting cultivation—a common agricultural practice in Mizoram—has led to deforestation and accelerated soil erosion, as reflected in declining NDVI values (Sengupta and Nath, 2022; Wilkinson et al., 2002).

Among the various landslide triggers, rainfall remains one of the most significant. Mizoram receives an annual average rainfall of 2,500–3,200 mm, with landslides peaking during the monsoon season (Sabatakakis et al., 2013). Intense and prolonged rainfall saturates the soil, weakening its structure and increasing the likelihood of slope failure. Additionally, Mizoram falls within Earthquake Zone V, where seismic activity poses an ongoing threat to slope stability (Sengupta and Nath, 2022). Other topographic features, such as slope gradient and wetness index, further influence landslide susceptibility (Catani et al., 2005; Shahabi et al., 2013). Steeper slopes are subjected to greater gravitational forces, making them more prone to failure (Devkota et al., 2013). Moreover, slopes exposed to prevailing winds and direct rainfall infiltration are particularly vulnerable to landslides (Yuke et al., 2022.; Zhang et al., 2021). Given Mizoram's rugged terrain, weak geological formations, heavy rainfall, and ongoing human activities, landslides continue to pose a major threat. Addressing this issue requires a comprehensive approach to risk assessment and mitigation, integrating scientific research with sustainable land-use planning to minimize the impact of these disasters.

### 2.3 Collinearity Test of Independent Factors

There are several methods for assessing collinearity in a dataset, with the correlation matrix and Variance Inflation Factor (VIF) being among the most commonly used. A correlation matrix, often visualized through a heat map, provides an overview of the relationships between variables by displaying their correlation coefficients. These coefficients range from -1 to 1, indicating both the strength and direction of the relationship. A value of -1 signifies a perfect negative correlation, meaning that as one variable increases, the other decreases. Conversely, a value of 1 indicates a perfect positive correlation, where both variables move in the same direction. A coefficient close to 0 suggests little to no correlation between the variables. Researchers frequently use correlation matrices to analyze variable interactions and detect potential multicollinearity (Saadatkhah et al., 2015).

Another widely used method for detecting multicollinearity is the Variance Inflation Factor (VIF), a statistical measure that quantifies how much a predictor variable is correlated with other independent variables in a regression model. High multicollinearity can distort coefficient estimates, making it difficult to interpret the model accurately. The VIF is calculated by dividing the variance of a predictor variable in the model by the variance it would have if it were completely uncorrelated with other predictors. A VIF value of 1 indicates no multicollinearity, while values greater than 1 suggest some level of correlation. In general, a VIF above 5 or 10 is considered problematic, as it suggests a strong correlation that could undermine the reliability of the model (Aversa et al., 2016.). The VIF is computed using the following equation:

$$VIF = \frac{1}{1-R^2} \quad (1)$$

where, $R^2$ is the coefficient of determination obtained by regressing the predictor variable against all other independent variables.

### 2.4 Machine Learning methods

The models were implemented in Python using Scikit-learn and XGBoost libraries. Hyperparameters were tuned using grid search techniques, and all raster datasets were standardized to a spatial resolution of 30 m × 30 m. To apply machine learning techniques effectively, a 50-meter buffer zone was created around the crown of each landslide point. This approach was based on the assumption that the most relevant and undisturbed morphological characteristics would be found in the area closest to the landslide. This concept, known as the "Seed Cell Theory," was first introduced by Suzen and Doyuran (2004), and is also referred to as the buffer zone method. To ensure an efficient transfer of attribute information, attribute values from the original data layer were assigned to the buffer zones using conversion points.

By applying the Seed Cell Theory, over 10,000 additional landslide points were generated. Non-landslide samples were generated outside the buffer zone using random point extraction. A range of machine learning models, including Random Forest (RF), Gradient Boosting Decision Tree (GBDT), and Extreme Boosting (XGB), were selected based on their reported performance in previous studies.

Additionally, these models were stacked with Logistic Regression (LR) to enhance classification accuracy. These algorithms were chosen for their ability to assign classification weights to various landslide parameters and their robust learning capabilities with parameter tuning.

The dataset used for training these models consisted of both landslide and non-landslide points, which were randomly divided into 80% training and 20% testing subsets. To assess the models' ability to accurately predict landslide-prone areas, specificity and sensitivity tests were performed using the Receiver Operating Characteristic (ROC) curve. The entire machine learning implementation was carried out using Python (Yuke et al., 2022).

### 2.5 Risk classification and interpretation

To assess population exposure in Mizoram, demographic data was gathered from government census records and GIS-based population density layers (Sengupta and Nath, 2022). This data was then overlaid with the landslide susceptibility map to identify areas where densely populated regions coincide with high-risk zones. A weighted scoring approach was used to assign higher risk ratings to locations falling within more susceptible categories, allowing for a comparative analysis of population exposure across different areas (Sengupta and Nath, 2022).

For infrastructure risk assessment, essential facilities such as buildings, roads, hospitals, and schools were mapped using GIS data. By analyzing the spatial distribution of infrastructure in relation to landslide-prone areas, it was possible to identify critical structures located within high and severe susceptibility zones (Yuke et al., 2022.). These locations were considered to have the highest infrastructure risk, as landslides in these areas could lead to major economic losses and social disruptions. The data analysis and visualization for this assessment were conducted using Python (Dou et al., 2020).

To systematically evaluate landslide risks across districts, a relative risk score was developed, incorporating both infrastructure vulnerability and population exposure. By normalizing the results and assigning composite scores, this evaluation helped highlight high-risk areas where mitigation efforts should be prioritized. A Relative Risk Index (RRI) was then introduced to quantify and compare landslide hazards across Mizoram's districts. This index was computed by weighing and normalizing two key factors: infrastructure vulnerability and population exposure, providing a comprehensive risk assessment for the region (Sengupta and Nath, 2022).

The computed RRI values were then categorized into different risk levels:

- Low Risk: $RRI<0.3$
- Moderate Risk: $0.3 \leq RRI<0.5$
- High Risk: $0.5 \leq RRI<0.7$
- Severe Risk: $RRI \geq 0.7$

## 3. Result and Discussion

### 3.1 Result from collinearity test

The Variance Inflation Factor (VIF) is a widely used metric for assessing the level of multicollinearity among predictor variables in a regression model. Generally, a VIF score above 5 is considered problematic, though any value greater than 1 suggests some degree of collinearity. In this study, as shown in Table 1, none of the predictor variables exceeded a VIF value of 5, indicating that multicollinearity is not a concern. This suggests that collinearity is unlikely to compromise the accuracy or interpretation of the regression results (Saadatkhah et al., 2015).

Additionally, the correlation matrix reveals that most conditioning factors fall within a range of -0.4 to 0.6, as illustrated in Figure 2. This indicates that each predictor variable contributes independently to the model's predictions and that strong dependencies between variables are minimal (Aversa et al., 2016.).

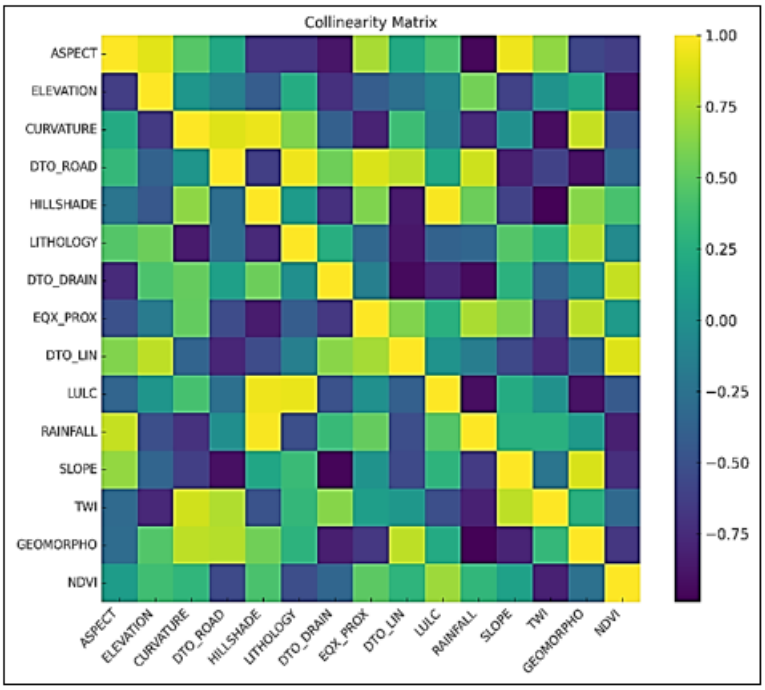


**Figure 2:** Multicollinearity assessment using correlation matrix

### 3.2 Analysis result of the model methods

Within a GIS framework, the Landslide Susceptibility Maps generated by the models were classified into five categories: low, moderate, high, very high, and severe. To validate the maps, historical landslide inventory data was used to determine what percentage of past landslide points fell within each susceptibility class. A map was considered suitable for risk modelling if at least 60% of historical landslide occurrences were located in the high to severe susceptibility zones. This approach is based on the assumption that future landslides are more likely to occur in areas with similar physiographic characteristics to those where past and present landslides have taken place.

To assess the performance of the six machine learning models, various evaluation metrics were applied, including Accuracy, Precision, Recall, F-measure, Area Under the ROC Curve (AUC), Mean Absolute Error (MAE), Root Mean Square Error (RMSE), and the Kappa Index (Yuke et al., 2022). A model was considered to perform better if it exhibited lower RMSE and MAE values while achieving higher Accuracy, Precision, Recall, F-measure, AUC, and Kappa Index scores. The results of this evaluation are presented in Tables 2 and 3.

According to Table 2, the XGB model demonstrated strong predictive capability, achieving the highest AUC value of 0.929, followed by GBDT and RF, both exceeding 0.900. When considering performance metrics, the XGB+LR model outperformed the others, obtaining the highest Accuracy, Precision, Recall, and F-measure values. In terms of error measures, the XGB+LR model had the lowest MAE and RMSE, while models like XGB, GBDT+LR, and XGB+LR showed high Kappa Index values, indicating the reliability and consistency of the Landslide Susceptibility Models (Yuke et al., 2022). Overall, the machine learning models demonstrated strong predictive accuracy, with XGB achieving the highest AUC of 0.929, followed by GBDT (0.927) and RF (0.907). Thus, the stacking ensemble approach proved effective in enhancing model performance. Among all the models analysed, XGB emerged as the most accurate.

The landslide susceptibility maps (LSM) generated by different machine learning models, based on historical landslide data, are presented in Figure 5 and the receiver Operator curve (ROC curves) was shown in fig. 4 for machine learning models as a representation of accuracy measurement.

The quality of the dataset plays a significant role in determining the accuracy of landslide prediction and risk assessment models. Interestingly, although stacking ensemble methods are expected to enhance performance, simple classifier models sometimes outperform them in AUC-based evaluations. Yuke et al. (2022) further argue that stacking models do not always guarantee better results than individual models, and a simple stacking approach may not necessarily improve predictive accuracy. However, when it comes to error reduction, the XGB+LR model outperformed all others, achieving the lowest MAE and RMSE and the highest Kappa Index, demonstrating its superior ability to minimize prediction errors.

**Table 1:** Multicollinearity calculation by VIF

| Sl No. | Factors | Variance Inflation Factor (Vif) |
|---|---|---|
| 1 | HILLSHADE | 1 |
| 2 | PROXIMITY TO EARTHQUAKE | 1 |
| 3 | ASPECT RATIO | 1 |
| 4 | DISTANCE TO LINEAMENT | 1 |
| 5 | GEOMORPHOLOGY | 1 |
| 6 | PLAN CURVATURE | 1 |
| 7 | DISTANCE TO DRAIN | 1 |
| 8 | LITHOLOGY | 1 |
| 9 | RAINFALL | 1 |
| 10 | LANDUSE/ LAND COVER (LULC) | 1 |
| 11 | SLOPE | 1 |
| 12 | TOPOGRAPHY WETNESS INDEX (TWI) | 1 |
| 13 | ELEVATION | 1 |
| 14 | NORMALIZED DIFFERENCE VEGETATION INDEX (NDVI) | 1.1 |
| 15 | DISTANCE TO ROAD | 1.1 |

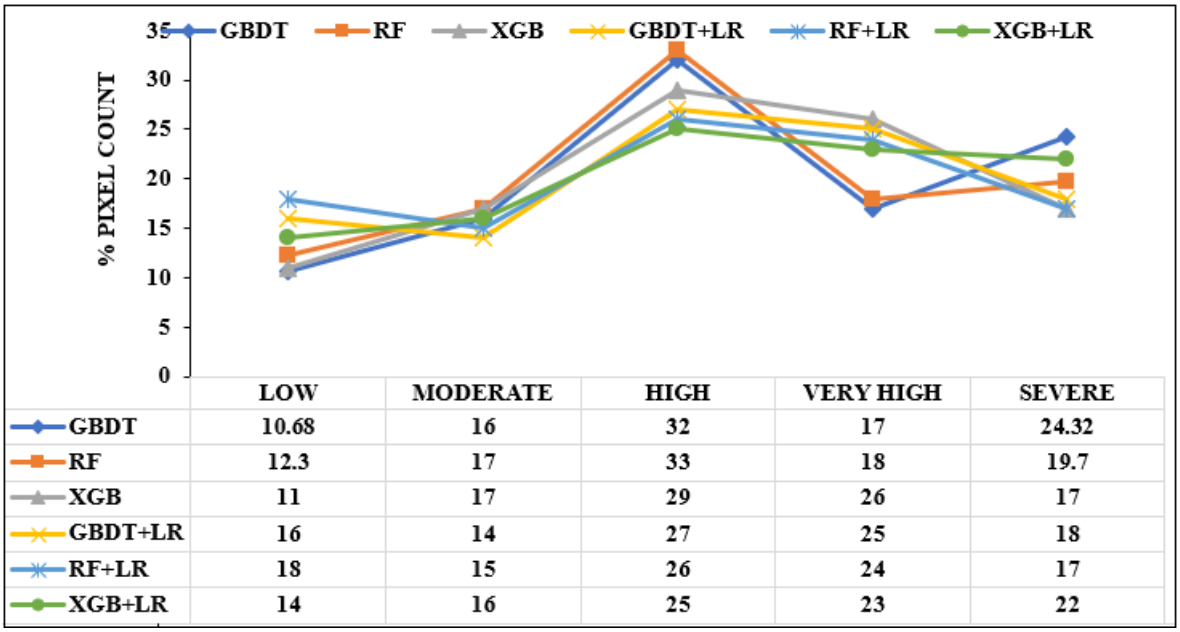


| | LOW | MODERATE | HIGH | VERY HIGH | SEVERE |
|---|---|---|---|---|---|
| GBDT | 10.68 | 16 | 32 | 17 | 24.32 |
| RF | 12.3 | 17 | 33 | 18 | 19.7 |
| XGB | 11 | 17 | 29 | 26 | 17 |
| GBDT+LR | 16 | 14 | 27 | 25 | 18 |
| RF+LR | 18 | 15 | 26 | 24 | 17 |
| XGB+LR | 14 | 16 | 25 | 23 | 22 |

**Figure 3:** Percentage distribution of landslide susceptibility classes derived from different machine learning models

**Table 2:** Assessment of landslide models using machine learning metrics

| Models | Accuracy | Precision | Recall | F-Measure | AUC |
|---|---|---|---|---|---|
| GBDT+LR | 0.914 | 0.983 | 0.998 | 0.9914 | 0.868 |
| RF+LR | 0.927 | 0.984 | 0.998 | 0.996 | 0.877 |
| XGB+LR | 0.981 | 0.987 | 0.999 | 0.992 | 0.89 |
| RF | 0.912 | 0.975 | 0.997 | 0.9882 | 0.907 |
| XGB | 0.955 | 0.981 | 0.998 | 0.9895 | 0.929 |
| GBDT | 0.923 | 0.965 | 0.998 | 0.9881 | 0.927 |

**Table 3:** Assessment of landslide models using error metrics

| MODELS | MAE | RMSE | KAPPA INDEX |
|---|---|---|---|
| GBDT+LR | 0.016 | 0.138 | 0.429 |
| RF+LR | 0.0189 | 0.139 | 0.39 |
| XGB+LR | 0.0157 | 0.124 | 0.576 |
| GBDT | 0.022 | 0.147 | 0.226 |
| RF | 0.0236 | 0.156 | 0.074 |
| XGB | 0.0197 | 0.147 | 0.523 |

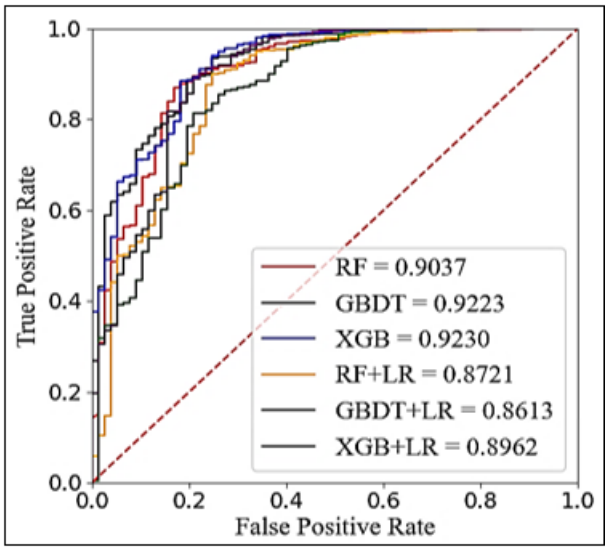


**Figure 4:** ROC curves of various machine learning landslide models

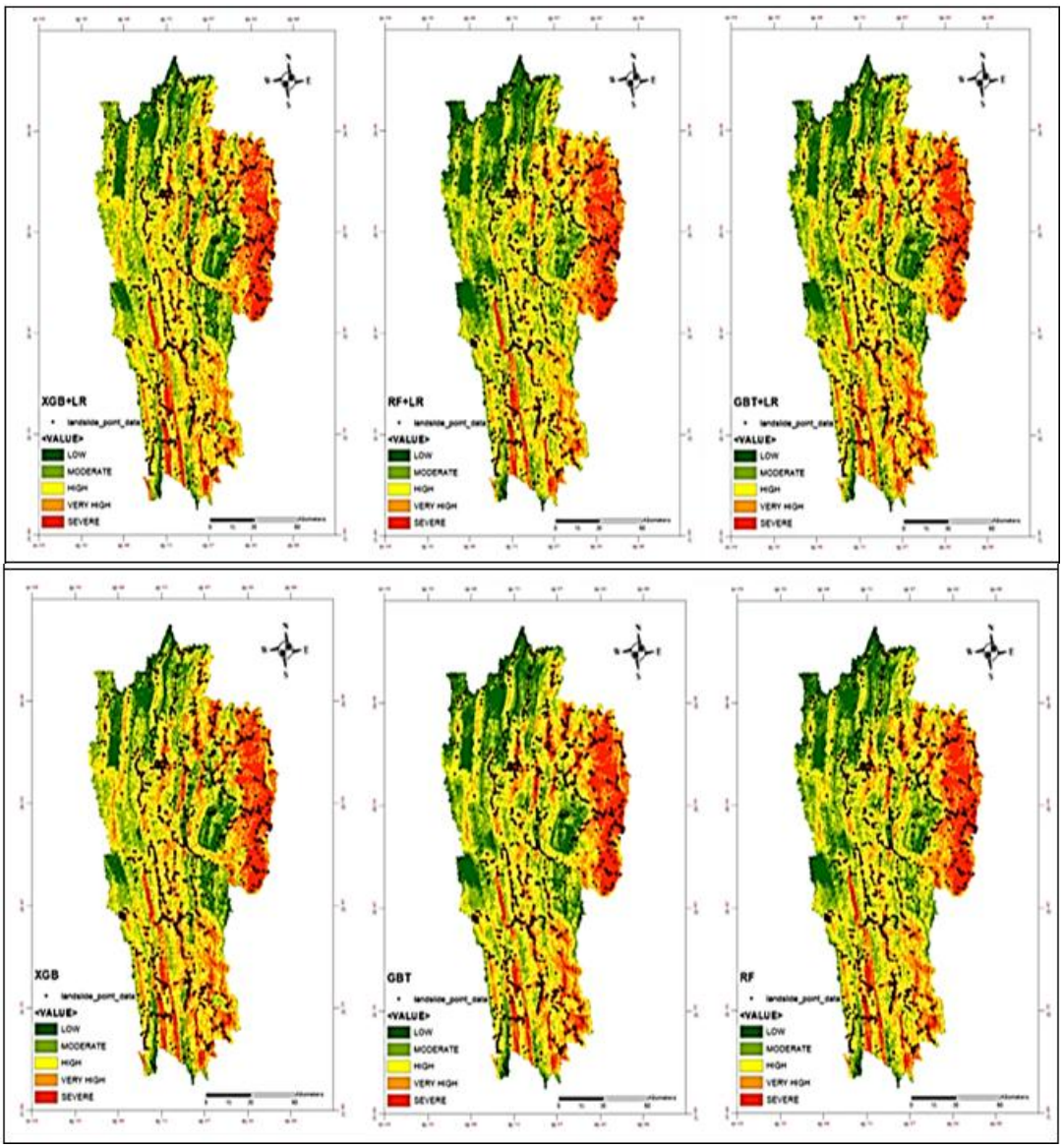


**Figure 5:** Landslide Susceptibility Maps of XGB+LR, RF+LR, GBDT+LR, XGB, GBDT and RF with historical landslide locations

### 3.3 Risk assessment from LSM

The Mizoram landslide susceptibility map may be used with population density and infrastructure data to determine danger levels in certain places. This method aids in evaluating the possible impact of landslides on human populations, transportation networks, and key infrastructure like hospitals and schools.

The population density in Mizoram varies significantly across different districts, influencing the extent to which landslides pose a direct threat to human lives. Aizawl has the highest population density (113 people/km²), followed by Kolasib (60 people/km²) and Champhai (39 people/km²), according to the 2011 Census. Other districts, such as Lunglei, Lawngtlai, and Mamit, have substantially lower populations, making them relatively less vulnerable to landslides in terms of direct human impact as shown in Fig. 6. However, lower population density does not always equate to lower risk, as certain low-density areas may still be at high risk if they contain critical settlements, economic centres, or transportation routes.

By overlaying landslide susceptibility data with population density distribution, risk levels can be categorized. High-risk zones include areas where both landslide susceptibility and population density are high. These areas include urban and semi-urban settlements in Aizawl and Champhai, where human exposure to landslides is the greatest. Moderate-risk zones are areas with moderate landslide susceptibility and medium population density, such as Kolasib and Lawngtlai, where fewer people are at risk, but landslides can still cause significant disruptions. Low-risk zones are sparsely populated areas, such as Mamit and Saiha, where landslides may not directly affect a large number of people, but they may still pose environmental and infrastructural threats.

#### 3.3.2 Risk Assessment Based on Infrastructure

Mizoram's steep and rugged terrain make infrastructure, including roads, bridges, power lines, and water supply networks, highly vulnerable to landslides. The presence of landslide-prone slopes along major transportation routes, such as NH-54, which connects Aizawl to Silchar, increases the likelihood of road blockages, supply chain disruptions, and delays in emergency response. Infrastructure-related landslide risks are not only concentrated in urban areas but also in rural locations where road networks and essential services may be affected by slope failures.

The classification of infrastructure risk is based on the exposure of critical infrastructure to landslide-prone areas. High-risk zones include locations where major road networks, power transmission lines, and water pipelines intersect with areas of high landslide susceptibility. Urban centers such as Aizawl are particularly at risk due to their dense infrastructure, steep slopes, and high development activity. Rural districts such as Champhai and Lawngtlai face moderate risk, as landslides could impact transportation and essential services, though the overall infrastructure concentration is lower compared to urban areas. The lowest-risk areas include districts like Saiha and Serchhip, where infrastructure development is minimal and landslide susceptibility is lower as shown in Fig. 7.

The combined analysis of landslide susceptibility, population density, and infrastructure risk indicates that urbanized and infrastructure-heavy districts such as Aizawl and Champhai are at the highest risk. In contrast, districts with lower development levels and fewer human settlements, such as Saiha and Serchhip, experience lower overall risk. However, even in less populated regions, damage to critical infrastructure could result in significant economic and logistical challenges. This assessment highlights the need for an integrated approach to landslide mitigation, incorporating geospatial analysis, machine learning predictions, and socioeconomic factors to develop effective risk reduction strategies.

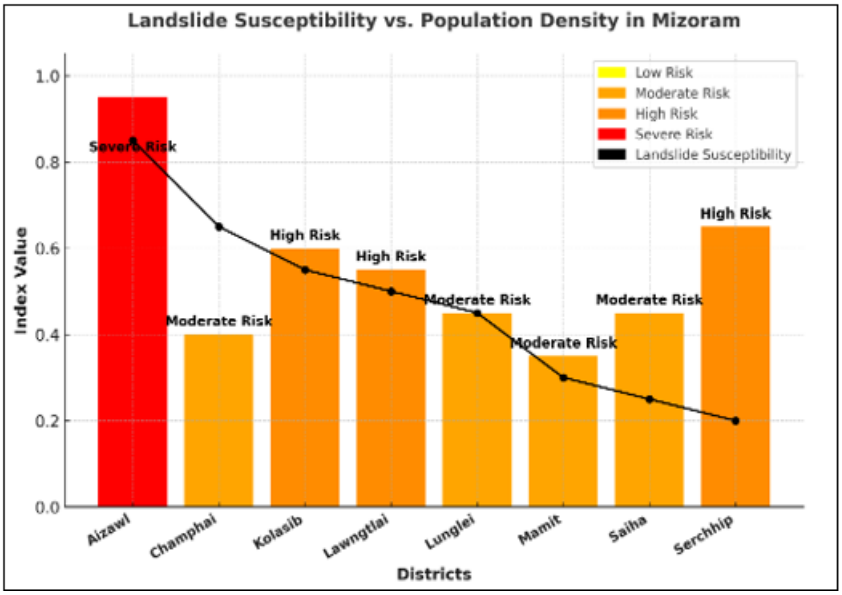


**Figure 6:** Correlation between LSM and population density risk of various district in Mizoram

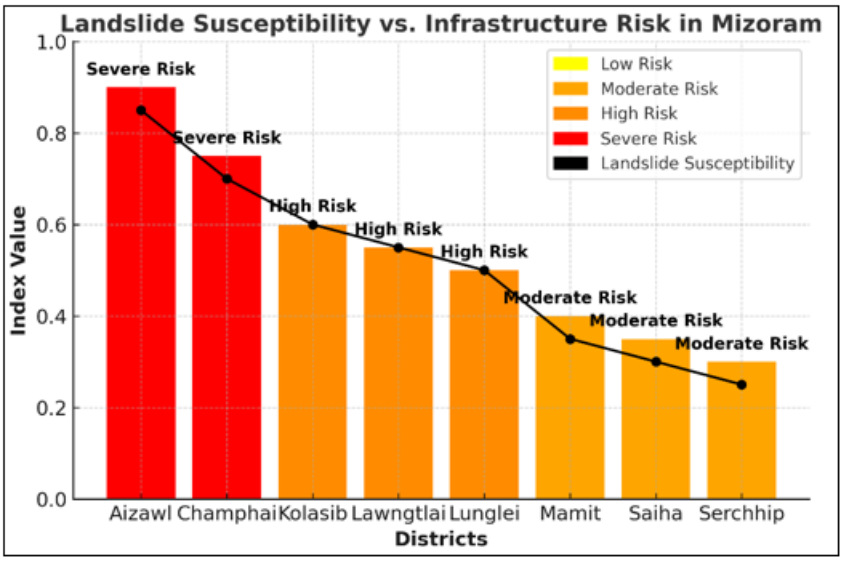


**Figure 7:** Correlation between LSM and infrastructure risk of various district in Mizoram

## 4. Conclusion

This study demonstrates the effectiveness of integrating GIS and machine learning techniques for landslide susceptibility assessment in Mizoram. Among the evaluated models, the XGB based approaches achieved the highest predictive performance with AUC values exceeding 0.90 and lower error metrics, confirming their reliability for hazard mapping. The incorporation of a 50 m buffer and seed cell approach enhanced dataset robustness and model training. The generated susceptibility maps, combined with population and infrastructure data, identified high risk districts such as Aizawl and Champhai. These findings provide a practical framework for targeted mitigation strategies, including early warning systems and improved land use planning. The study contributes to advancing data driven disaster risk management and supports the development of resilient infrastructure in landslide prone regions.

**Author Contributions:**
Satyaprakash: Conceptualization, Methodology, Supervision, Writing – Review & Editing.
Joel TC Vanlalnunzira: Data Curation, Formal Analysis, Investigation, Software, Visualization, Writing – Original Draft.
Both authors contributed to the interpretation of results and approved the final manuscript.

**Statements and Declaration**

**Funding:** The authors declare that no funds, grants, or other support were received during the preparation of this manuscript.

**Competing Interests:** The authors declare no competing interest.

**Ethical Approval:** The present study does not include any testing on humans or animals hence no ethical approval was sought from any agency. The data was collected from sources which are open to everyone and was collected as per our institution's Ethical Review Guidelines.

**Consent to Participate:** Since no tests were performed on humans or animals, no consent was obtained to participate in the research.

**Consent to Publish:** Informed consent was obtained from all the authors before the publication of research findings.

## References

[1] Alejandrino, I.K., Lagmay, A.M., Eco, R.N., 2016. Shallow landslide hazard mapping for Davao Oriental, Philippines, using a deterministic GIS model, in: Advances in Natural and Technological Hazards Research. Springer Netherlands, pp. 131–147. https://doi.org/10.1007/978-3-319-20161-0_9

[2] Aversa, S., Cascini, L., Picarelli, L. (Luciano), Scavia, C. (Claudio), 2016. Landslides and engineered slopes. experience, theory and practice : proceedings of the 12th International Symposium on Landslides (Napoli, Italy, 12-19 June 2016).

[3] Bhusan, K., Singh, M.S., Sudhakar, S., 2013. Landslide hazard zonation using RS and GIS techniques: A case study from north east India, in: Landslide Science and Practice: Landslide Inventory and Susceptibility and Hazard Zoning. Springer Science and Business Media Deutschland GmbH, pp. 489–492. https://doi.org/10.1007/978-3-642-31325-7_63

[4] Catani, F., Casagli, N., Ermini, L., Righini, G., Menduni, G., 2005. Landslide hazard and risk mapping at catchment scale in the Arno River basin. Landslides 2, 329–342. https://doi.org/10.1007/s10346-005-0021-0

[5] Dai, F.C., Lee, C.F., 2002. Landslide characteristics and slope instability modeling using GIS, Lantau Island, Hong Kong. Geomorphology 42, 213–228. https://doi.org/10.1016/S0169-555X(01)00087-3

[6] Devkota, K.C., Regmi, A.D., Pourghasemi, H.R., Yoshida, K., Pradhan, B., Ryu, I.C., Dhital, M.R., Althuwaynee, O.F., 2013. Landslide susceptibility mapping using certainty factor, index of entropy and logistic regression models in GIS and their comparison at Mugling–Narayanghat road section in Nepal

Himalaya. Natural Hazards 65, 135–165. https://doi.org/10.1007/s11069-012-0347-6

[7] Dou, J., Yunus, A.P., Bui, D.T., Merghadi, A., Sahana, M., Zhu, Z., Chen, C.-W., Han, Z., Pham, B.T., 2020. Improved landslide assessment using support vector machine with bagging, boosting, and stacking ensemble machine learning framework in a mountainous watershed, Japan. Landslides 17, 641–658. https://doi.org/10.1007/s10346-019-01286-5

[8] Huang, M., Fielding, E.J., Liang, C., Milillo, P., Bekaert, D., Dreger, D., Salzer, J., 2017. Coseismic deformation and triggered landslides of the 2016 $M_w$ 6.2 Amatrice earthquake in Italy. Geophys. Res. Lett. 44, 1266–1274. https://doi.org/10.1002/2016GL071687

[9] Nefeslioglu, H.A., Duman, T.Y., Durmaz, S., 2008. Landslide susceptibility mapping for a part of tectonic Kelkit Valley (Eastern Black Sea region of Turkey). Geomorphology 94, 401–418. https://doi.org/10.1016/j.geomorph.2006.10.036

[10] Pourghasemi, H.R., Mohammady, M., Pradhan, B., 2012. Landslide susceptibility mapping using index of entropy and conditional probability models in GIS: Safarood Basin, Iran. Catena (Amst). 97, 71–84. https://doi.org/10.1016/j.catena.2012.05.005

[11] Pradhan, B., 2010. Landslide susceptibility mapping of a catchment area using frequency ratio, fuzzy logic and multivariate logistic regression approaches. Journal of the Indian Society of Remote Sensing 38, 301–320. https://doi.org/10.1007/s12524-010-0020-z

[12] Saadatkhah, N., Kassim, A., Min Lee, L., Yunusa, G.H., 2015. Quantitative Hazard Analysis for Landslides in Hulu Kelang area, Malaysia. J. Teknol. 73. https://doi.org/10.11113/jt.v73.2977

[13] Sabatakakis, N., Koukis, G., Vassiliades, E., Lainas, S., 2013. Landslide susceptibility zonation in Greece. Natural Hazards 65, 523–543. https://doi.org/10.1007/s11069-012-0381-4

[14] Sengupta, A., Nath, S.K., 2022. GIS-Based Landslide Susceptibility Mapping in Eastern Boundary Zone of Northeast India in Compliance with Indo-Burmese Subduction Tectonics, in: Advances in Geographic Information Science. Springer Science and Business Media Deutschland GmbH, pp. 19–37. https://doi.org/10.1007/978-3-030-75197-5_2

[15] Shahabi, H., Ahmad, B.B., Khezri, S., 2013. Evaluation and comparison of bivariate and multivariate statistical methods for landslide susceptibility mapping (case study: Zab basin). Arabian Journal of Geosciences 6, 3885–3907. https://doi.org/10.1007/s12517-012-0650-2

[16] Süzen, M.L., Doyuran, V., 2004. Data driven bivariate landslide susceptibility assessment using geographical information systems: a method and application to Asarsuyu catchment, Turkey. Eng. Geol. 71, 303–321. https://doi.org/10.1016/S0013-7952(03)00143-1

[17] Thai Pham, B., Tien Bui, D., Prakash, I., 2018. Landslide susceptibility modelling using different advanced decision trees methods. Civil Engineering and Environmental Systems 35, 139–157. https://doi.org/10.1080/10286608.2019.1568418

[18] Tien Bui, D., Pradhan, B., Lofman, O., Revhaug, I., Dick, O.B., 2012. Spatial prediction of landslide hazards in Hoa Binh province (Vietnam): A comparative assessment of the efficacy of evidential belief functions and fuzzy logic models. Catena (Amst). 96, 28–40. https://doi.org/10.1016/j.catena.2012.04.001

[19] Wilkinson, P.L., Anderson, M.G., Lloyd, D.M., 2002. An integrated hydrological model for rain-induced landslide prediction. Earth Surf. Process. Landf. 27, 1285–1297. https://doi.org/10.1002/esp.409

[20] Yalcin, A., Bulut, F., 2007. Landslide susceptibility mapping using GIS and digital photogrammetric techniques: A case study from Ardesen (NE-Turkey). Natural Hazards 41, 201–226. https://doi.org/10.1007/s11069-006-9030-0

[21] Yuke, H., Khan, U., Zhang, B., Huan, Y., Song, L., 2022. Stacking Ensemble of Machine Learning Methods for Landslide Susceptibility Mapping in Zhangjiajie City, Hunan Province, China Bayesian-MCMC Inference of Geochemical Fields Constrained by Three-dimensional Geological Model View project 3D Geosciences Spatial Field Modeling in Consideration of Geological Occurrence View project Stacking ensemble of machine learning methods for landslide susceptibility mapping in Zhangjiajie City, Hunan Province, China. https://doi.org/10.20944/202203.0337

[22] Zhang, J., Zhu, W., Cheng, Y., Li, Z., 2021. Landslide detection in the linzhi–ya'an section along the sichuan–tibet railway based on insar and hot spot analysis methods. Remote Sens. (Basel). 13. https://doi.org/10.3390/rs13183566

[23] Zhu, L., Huang, J., 2006. GIS-based logistic regression method for landslide susceptibility mapping in regional scale. Journal of Zhejiang University-SCIENCE A 7, 2007–2017. https://doi.org/10.1631/jzus.2006.A2007